Glycobiology vol. 18 no. 1 pp. 84–96, 2008
doi:10.1093/glycob/cwm122
Advance Access publication on October 30, 2007

Glycosylinositolphosphoceramides in *Aspergillus fumigatus*

Catherine Simenel[2], Bernadette Coddeville[3], Muriel Delepierre[2], Jean-Paul Latgé[4], and Thierry Fontaine[1,4]

[2]Unité de Résonance Magnétique Nucléaire des Biomolécules, CNRS URA 2185 Institut Pasteur, 25 rue du Docteur Roux 75724 Paris cedex 15; [3]Unité de Glycobiologie Structurale et Fonctionnelle, UMR 8576 CNRS, Université des Sciences et Technologies de Lille, 59655 Villeneuve d'Ascq cedex; and [4]Unité des Aspergillus, Institut Pasteur, 25 rue du Docteur Roux 75724 Paris cedex 15, France

Received on August 01, 2007; revised on October 23, 2007; accepted on October 23, 2007

Fungal glycosylinositolphosphoceramides (GIPCs) are involved in cell growth and fungal–host interactions. In this study, six GIPCs from the mycelium of the human pathogen *Aspergillus fumigatus* were purified and characterized using Q-TOF mass spectrometry and ^{1}H, ^{13}C, and ^{31}P NMR. All structures have the same inositolphosphoceramide moiety with the presence of a $C_{18:0}$-phytosphingosine conjugated to a 2-hydroxylated saturated fatty acid (2-hydroxylignoceric acid). The carbohydrate moiety defines two types of GIPC. The first, a mannosylated zwitterionic glycosphingolipid contains a glucosamine residue linked in α1-2 to an inositol ring that has been described in only two other fungal pathogens. The second type of GIPC presents an α-Manp-(1→3)-α-Manp-(1→2)-IPC common core. A galactofuranose residue is found in four GIPC structures, mainly at the terminal position via a β1-2 linkage. Interestingly, this galactofuranose residue could be substituted by a choline–phosphate group, as observed only in the GIPC of *Acremonium sp.*, a plant pathogen.

Keywords: Aspergillus fumigatus/galactofuranose/glycosphingolipid/glycosylinositolphosphoceramide/NMR

Introduction

Glycosphingolipids (GSLs) are membrane glycolipids found in all eukaryotic cells that are composed of a carbohydrate and a ceramide hydrophobic moiety. In yeast and fungi, three types of GSLs have been identified. The first class is represented by neutral β-glucosyl-ceramide and β-galactosyl-ceramide. This type of GSL plays a crucial role in spore germination, hyphal growth, and in the cell cycle (Levery et al. 2002; Barreto-Bergter et al. 2004; da Silva et al. 2004; Rittershaus et al. 2006). The second class of fungal GSLs is composed of a complex neutral moiety and a saturated ceramide, suggesting a different biosynthetic pathway (Maciel et al. 2002; Aoki, Uchiyama, Yamauchi et al. 2004; Barreto-Bergter et al. 2004). The third class is composed of glycosylinositolphosphoceramides (GIPCs) which are acidic GSLs containing a phosphodiester linkage between inositol and ceramide. In contrast to cerebrosides, these phosphorylinositol-containing sphingolipids are not present in mammals but have been detected in protozoa, plants, fungi, and nematodes. The sphingolipids are essential for fungal growth since the deletion of inositolphosphorylceramide (IPC) synthase that catalyzes the transfer of inositol and phosphate to ceramide is lethal in *Saccharomyces* and *Aspergillus* (Nagiec et al. 1997; Cheng et al. 2001; Hu et al. 2007). In filamentous fungi, the ceramide moiety is composed of a phytosphingosine associated with a saturated long chain fatty acid containing 18 to 26 carbon atoms with or without a hydroxyl group in position 2. The carbohydrate moiety is more variable. Three types of GIPCs have been mainly identified based on the monosaccharide and its linkage to the inositol ring: (i) α-Man-(1-2)-IPC found in numerous species (Barr et al. 1984; Levery et al. 1998, 2001; Heise et al. 2002), (ii) α-Man-(1-6)-IPC found in *Sporothrix schenckii* (Loureiro y Penha et al. 2001; Toledo, Levery, Glushka et al. 2001), and (iii) α-GlcN-(1-2)-IPC described in *S. schenckii, Acremonium sp.*, and *Aspergillus fumigatus* (Toledo, Levery, Straus et al. 2001; Toledo et al. 2007; Aoki, Uchiyama, Itonori et al. 2004). To these core structures, other monosaccharides such as fucose, xylose, galactose, or choline–phosphate could be associated (Jennemann et al. 1999; Heise et al. 2002; Arigi et al. 2007; Gutierrez et al. 2007). The presence of an α-Man-(1-4)-IPC sequence has only been reported in Basidiomycetes, outside the three families described suggesting a high level of complexity in the structure of the fungal sphingolipids (Jennemann et al. 2001).

A. fumigatus is a saprophytic, filamentous fungus found in most environments where it plays an important role in the recycling of organic materials. *A. fumigatus* is also an opportunistic pathogen responsible for severe pulmonary diseases, particularly in immunocompromised patients (Latgé 1999). Man_2-IPC and five other GIPC structures containing additional mannose, galactofuranose, glucosamine, or *N*-acetylglucosamine residues have been previously identified in *A. fumigatus* (Levery et al. 2001; Toledo et al. 2007). This fungus also produces a lipogalactomannan linked to the cellular membrane through a GlcN-IPC (Costachel et al. 2005). As an effort to identify cell surface glycans and antigens, four new structures of GIPC were isolated from membrane preparations of *A. fumigatus* mycelium and chemically characterized using mass spectrometry and NMR analysis.

Results

The crude membrane preparation of *A. fumigatus* mycelium was treated with chloroform/methanol/water, then with a butanol/water partition to recover a glycolipid preparation. Two liquid chromatographic steps on a DEAE-Sephadex column and Silica 60 column were used to separate five glycosphingolipid

[1]To whom correspondence should be addressed: e-mail: tfontain@pasteur.fr

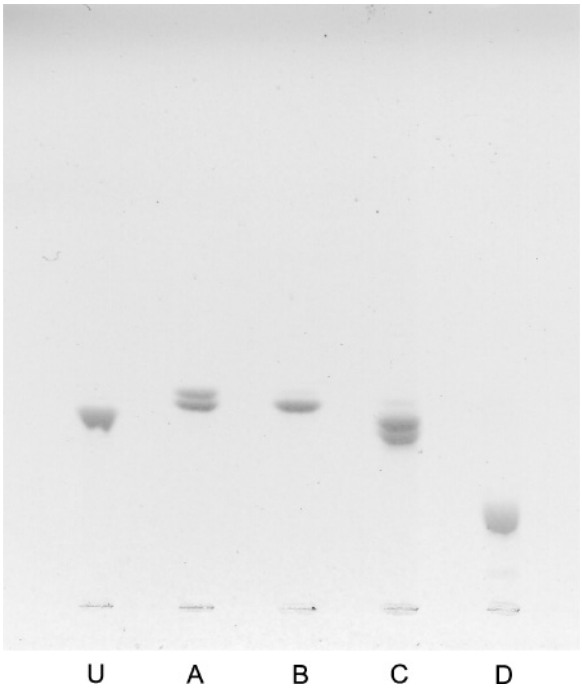

Fig. 1. HPTLC of GSL fractions (U, A, B, C, and D) isolated from *A. fumigatus* mycelium. TLC was developed on 10-cm aluminum-coated silica gel 60 with chloroform/methanol/1 M ammonium acetate/NH_4OH 30%/water (180/140/9/9/23). Sugars were detected using orcinol sulfuric acid.

fractions (Figure 1). The total amount of GSLs represented around 0.02% ± 0.005 of the total mycelium dry weight. DEAE anion exchange chromatography yielded an unbound glycosphingolipid (GSL-U) and negatively charged GSLs. Similar amounts of unbound and bound fractions were purified from a 15-L fermentor in the Sabouraud medium of *A. fumigatus*. Silica gel column chromatography was used to purify the unbound GSL-U and four fractions of negatively charged GSLs (GSL-A, GSL-B, GSL-C, and GSL-D) (Figure 1). The GSL-A and GSL-C fractions contain two molecules. Only one spot was detected in fractions B and D.

Composition analysis obtained by GLC and GLC-MS revealed the presence of $C_{18:0}$-phytosphingosine and a 2-monohydroxylated $C_{24:0}$ fatty acid in all GSL fractions. Minor fatty acids such as 2OH-$C_{25:0}$ and 2OH-$C_{26:0}$ were observed in low amounts (data not shown). Mannose and *myo*-inositol were identified in all GSL fractions, whereas glucosamine was detected only in the GSL-U fraction and galactose only in negatively charged GSL fractions (GSL-A to D) (Table I).

GSL fractions have been analyzed by Q-TOF mass spectrometry to identify the molecular weight of isolated glycosphingolipids; pseudomolecular negative ions m/z are presented in Table I and Figure 2. The pseudomolecular ion at $m/z = 1410$ obtained with GSL-U fraction corresponded to a glycosphingolipid containing two hexose residues and one hexosamine associated with an inositolphosphoceramide (IPC) whereas the ceramide was composed of a $C_{18:0}$-phytosphingosine associated with a 2-hydroxylated $C_{24:0}$ fatty acid (Costachel et al. 2005). The presence of minor ions that differ by a mass of 14 or 28 reflected the variability in the size of fatty acids. Pseudomolecular ions at $m/z = 1249$, 1411, 1573, obtained with GSL-A, B, C fractions were compatible with a similar IPC with the presence of two, three, or four hexose residues. A fragmentation pseudomolecular ion at $m/z = 1411$ produced one main ion at $m/z = 745$ [Hex_3-inositol-phosphate]$^-$, ions at $m/z = 241$ and 259 corresponding to inositol–phosphate, and ions at $m/z = 79$ and 97 corresponding to free phosphate (Figure 2; Costachel et al. 2005). Fragmentation of pseudomolecular ions at $m/z = 1249$, 1411, 1573 gave similar patterns of fragmentation with the loss of 666 corresponding to the ceramide moiety (data not shown), characterizing a GIPC and indicating the presence of two, three, and four hexose residues linked to IPC. In contrast, the fragmentation of a pseudomolecular ion at $m/z = 1576$ in the GSL-D fraction did not produce similar patterns of daughter ions, indicating structural modifications (Figure 2). The composition of this GSL-D fraction indicated the presence of the same IPC structure with mannose residues. Indeed, a pseudomolecular mass at $m/z = 1576$ did not correspond to a classical mannosylated IPC, but instead, the presence of a choline–phosphate linked to a Hex_3-IPC. Daughter fragments at m/z 1517 [CH_2-CH_2-P-Hex_3-IPC]$^-$, 910 [$(CH_3)_3$N-CH_2-CH_2-P-Hex_3-inositol-P]$^-$, and 851 [CH_2-CH_2-P-Hex_3-inositol-P]$^-$ were in agreement with the presence of a choline–phosphate substituent. Moreover, GLC-MS analysis of the sugar–phosphate following methanolysis and trimethylsilylation of the GSL-D fraction permitted the identification of a monosaccharide-6-phosphate with the same retention time as the galactose-6-phosphate obtained from the lipophosphoglycan of *Leishmania donovani* (data not shown). These data suggest the presence of phosphocholine linked to the C6 of a galactose residue in the GSL-D fraction.

Linkages of monosaccharides were analyzed after methylation (Table II). Methylation of the GSL-U fraction revealed the presence of three methyl ethers corresponding to a terminal mannose, a mannose substituted in position 3, and a glucosamine

Table I. Carbohydrate composition and Q-TOF mass analysis of GSL fractions isolated from *A. fumigatus* mycelium (Man: mannose; Gal: galactose; GlcN: glucosamine; IPC: inositolphosphoceramide; Hex: hexose; Cho-P: choline-phosphate)

	Monosaccharide composition[a]				Pseudomolecular ions identified by Q-TOF		
GSL Fractions	Man	Gal	GlcN	Inositol	Main ions	Corresponding structures	Minor ions
GSL-U	1	–	0.49	+	1409.8	Hex_2-GlcN-IPC	1424.1; 1437.8
GSL-A	1	0.36	–	+	1249.1; 1411.2	Hex_2-IPC	1263.1; 1277.1
						Hex_3-IPC	1425.2; 1439.2
GSL-B	1	0.49	–	+	1411.2	Hex_3-IPC	1425.2; 1439.2
GSL-C	1	0.42	–	+	1573.3	Hex_4-IPC	1587.3; 1601.3
GSL-D	1	0.11	–	+	1576.3	Cho-P-Hex_3-IPC	1590.3; 1604.4

[a]Obtained by GC after hydrolysis with TFA (4 N, 100°C, 4 h) for neutral monosaccharides and HCl (6 N, 110°C 20 h) for glucosamine and inositol residues.

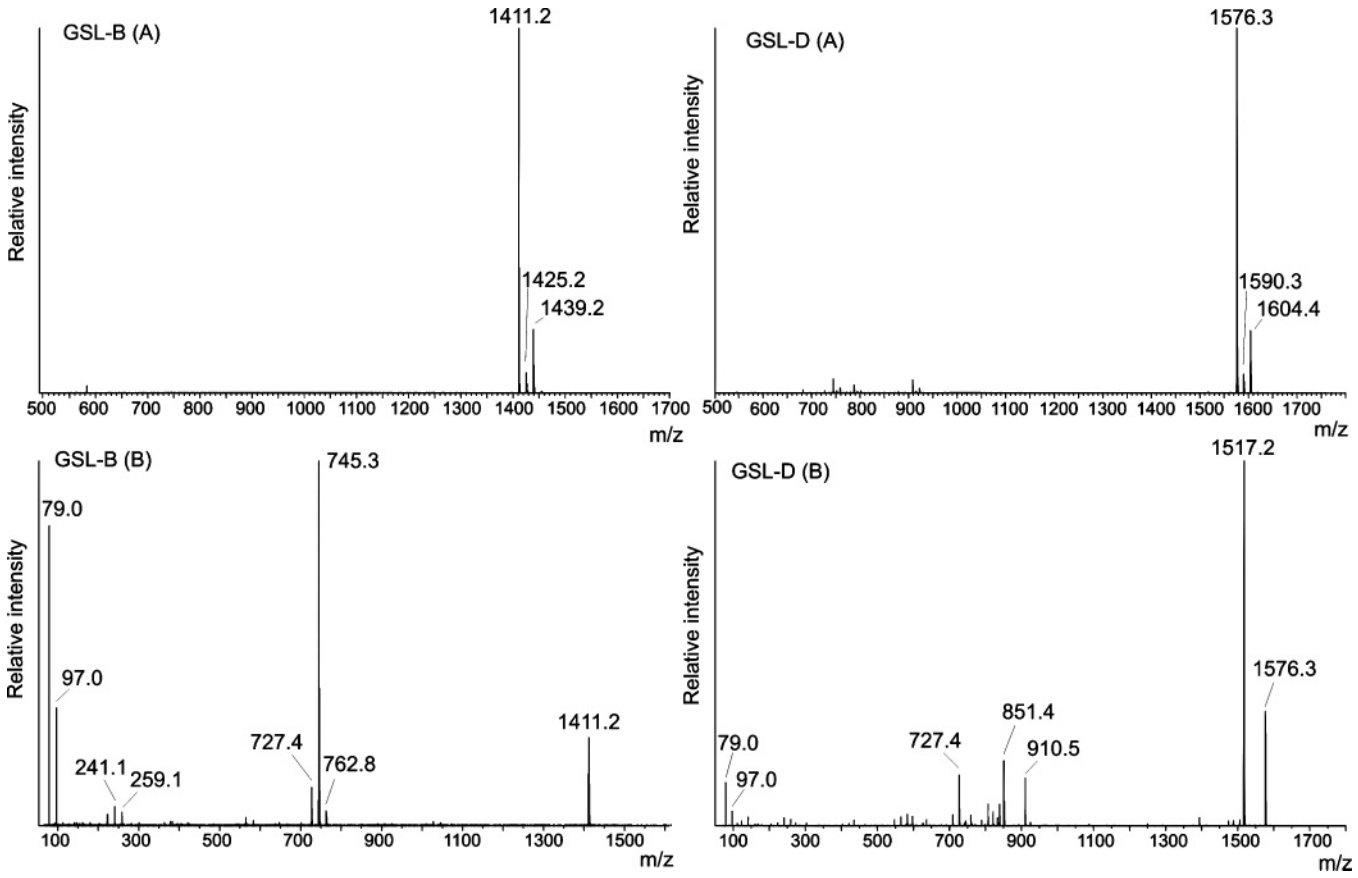

Fig. 2. Nanoelectrospray mass spectrometry analysis of GSL-B and GSL-D fractions of *A. fumigatus* mycelium. Mass spectrometric analyses were performed in the negative mode using a Q-STAR Pulsar quadrupole time-of-flight (Q-TOF) mass spectrometer equipped with a nanoelectrospray ion source. A: negative ion mass spectrum; B: daughter ion mass spectrum of molecular ion.

Table II. Molar ratio of methyl ethers obtained after permethylation of GIPC fractions isolated from *A. fumigatus* mycelium. Molar ratios were calculated by GLC-flame ionization detection after hydrolysis (TFA, 4 N, 6 h, 100°C) reduction with $NaBD_4$ and acetylation.

		Glycosphingolipid fractions				
Methyl ethers[a]	Linkages	GSL-U	GSL-A	GSL-B	GSL-C	GSL-D
2,3,4,6-Man	Man-	1.3	1.1	0.1	0.7	–
2,3,5,6-Gal	Gal_f-	–	0.8	0.7	1.1	–
3,4,6-Man	-2-Man-	–	1	1	1	1
2,4,6-Man	-3-Man-	1	1.6	0.7	–	1.1
2,4-Man	-3-^{6}Man-	–	–	–	0.8	–
2,3,5-Gal	-6-Gal_f-	–	–	–	–	+[b]
2,3,4-GlcNAc	-6-GlcN-	0.4	–	–	–	–

[a]Numbers indicate the position of methyl groups.
[b]This methyl ether was observed after hydrolysis by HCl 4 N, 4 h, 100°C.

substituted in position 6. In agreement with Q-TOF mass spectra and to GSL described in fungal species (Toledo, Levery, Straus et al. 2001; Toledo et al. 2007; Aoki, Uchiyama, Itonori et al. 2004), these data suggest the following sequence: Man1–3-Man1–6GlcN. In the GSL-A fraction, the presence of two terminal monosaccharides, a mannose and a galactofuranose, without a disubstituted monosaccharide confirmed the presence of two GSL structures. GSL-B fraction contained three major methyl ethers with a terminal galactofuranose, indicating, in agreement with the Q-TOF mass spectra, a Gal–Man–Man sequence. In the GSL-C fraction, a disubstituted mannose in positions 3 and 6 indicated a branched structure with a terminal galactofuranose and/or mannose. In the GSL-D fraction, two main methyl ethers corresponding to monosubstituted mannoses have been identified, but no terminal monosaccharide. A stronger acid hydrolysis yielded a 2,3,5-tri-*O*-methyl hexitol that should correspond to a galactofuranose substituted in position 6 by a phosphate identified after methanolysis and trimethysilylation. In agreement with the Q-TOF mass spectra (Figure 2), these data suggest a choline–phosphate–6-Galf–Man–Man sequence.

NMR analysis of the five glycosphingolipid fractions

The GSL structures of *A. fumigatus* mycelium were elucidated by analysis of homonuclear and heteronuclear two-dimensional NMR experiments.

In agreement with GLC and MS data (Table I), NMR analysis confirmed the presence of an identical ceramide structure in all GSL fractions. From signal integration in the 1D spectrum of the highest concentrated GSL-B fraction, the total number of carbons of the two aliphatic chains was estimated to be 42. A methylene/methyl ratio of 17.5 was in agreement with a $C_{18:0}$ phytosphingosine linked to an unbranched 2-hydroxylated $C_{24:0}$ fatty acid identified by GLC-MS. The carbon linked to

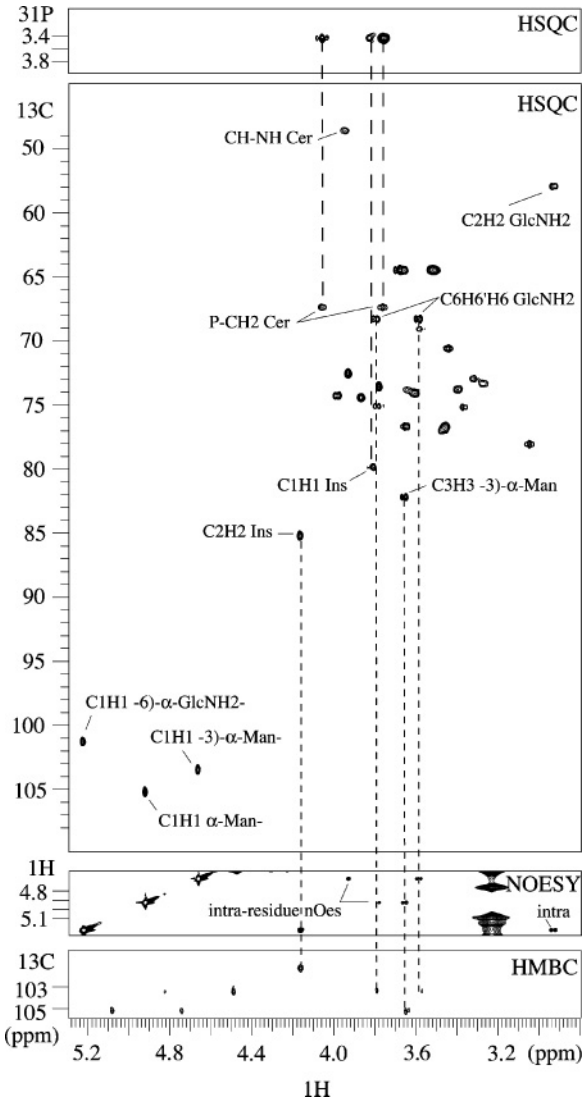

Fig. 3. NMR spectra of GSL-U isolated from *A. fumigatus* mycelium. ^{1}H-^{13}C HSQC, ^{1}H-^{1}H NOESY, ^{1}H-^{13}C HMBC, and ^{1}H-^{31}P HSQC.

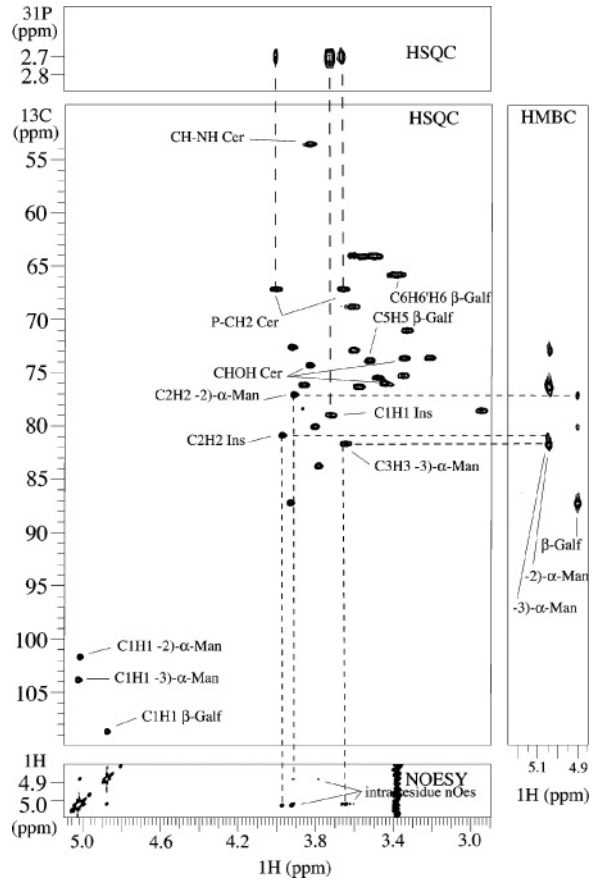

Fig. 4. NMR spectra of GSL-B from *A. fumigatus* mycelium. ^{1}H-^{13}C HSQC, ^{1}H-^{1}H NOESY, ^{1}H-^{13}C HMBC, and ^{1}H-^{31}P HSQC.

the nitrogen atom in the sphingosine base shifted at 53.36 ppm was located in the ^{1}H ^{13}C HSQC experiment as well as three ^{1}H/^{13}C shifts corresponding to CHOH groups at 3.451/76.01, 3.348/73.65, and 3.835/74.3 (Figure 4). A phosphorus atom was detected in the ceramide moiety attached to the glycosidic one. Indeed, three correlations were observed in the ^{1}H, ^{31}P HSQC spectrum between the phosphorus atom and two methylene protons of the ceramide on one side and the H1 proton of inositol on the other side (Figures 3–5) indicating the sequence inositol–P–ceramide.

GSL-U Fraction. The chemical shifts and coupling constants of the glycosidic moiety obtained for the GSL-U fraction are shown in Table III. The 1D ^{1}H and 2D ^{1}H, ^{13}C gHSQC spectra showed three signals in the anomeric region, in equal proportions as deduced from integration in the 1D spectrum, indicating the presence of three monosaccharide residues (Figure 3). The ^{1}H and ^{13}C chemical shift analysis and the examination of $^{3}J_{H,H}$ and $^{1}J_{C1,H1}$ values indicated the presence of two α-mannopyranose and one α-glucosamine residues (Bock and Pedersen 1974, 1983). The *myo*-inositol residue was identified from its H2 equatorial proton in the 1,2,3,4,5,6-cyclohexanehexol ring as assessed by the small $^{3}J_{H1,H2}$ and $^{3}J_{H2,H3}$ values (2.7 Hz) (Table III).

A NOESY experiment demonstrated a strong correlation between the H1 proton of a mannose residue and the H3 proton of the second mannose residue (Figure 3). Moreover, C1/H3 and H1/C3 correlations between these two mannose residues were observed in the gHMBC experiment (Figure 3), indicating a branched sequence of α-Manp-(1→3)-α-Manp. This sequence accounts for the downfield chemical shift of the C3 at 82.24 ppm of the second mannose residue (Table III). Similarly, dipolar interactions between the H1 proton of the second mannose residue and H6/H6′ protons of the glucosamine residue were observed in the NOESY experiment suggesting a →3)-α-Manp-(1→6)-α-GlcNH$_2$ sequence. This linkage was confirmed by a gHMBC experiment with the observation of the correlations H1/C6 and C1/H6H6′ between the second mannose residue and the glucosamine residue. This is in agreement with a C6 downfield chemical shift at 68.29 ppm observed for the glucosamine residue. A strong interaction was also observed in the NOESY experiment between the anomeric proton of the glucosamine residue and the H2 proton of the inositol residue, corroborated by the presence of a correlation between the C1

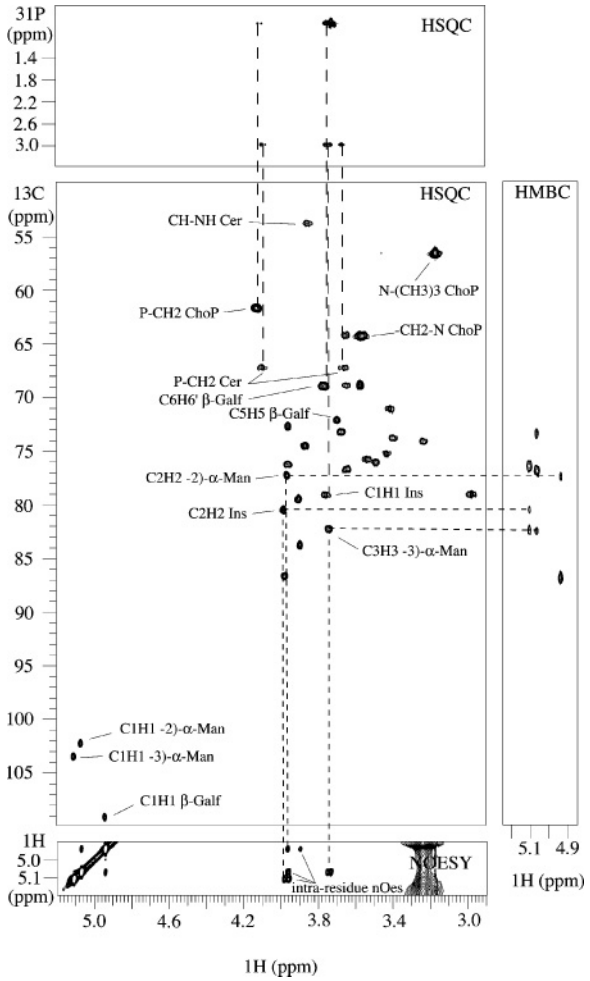

Fig. 5. NMR spectra of GSL-D from *A. fumigatus* mycelium. ^{1}H-^{13}C HSQC, ^{1}H-^{1}H NOESY, ^{1}H-^{13}C HMBC, and ^{1}H-^{31}P HSQC.

carbon of the glucosamine residue and the H2 proton of the inositol residue in the gHMBC experiment, indicating the sequence motif: →6)-α-GlcNH$_2$-(1→2)-Ins, in agreement with the downfield shift at 85.22 ppm of the inositol C2 carbon. Along with the MS data, the NMR experiments established the following structure: α-Manp-(1→3)-α-Manp-(1→6)-α-GlcNH$_2$-(1→2)-Ins-(1→O)-P-Cer. This structure has previously been characterized by NMR (Toledo et al. 2007). Differences in ^{1}H and ^{13}C chemical shifts are observed with our results that are associated primarily with the following: (i) the ^{13}C referencing method inducing a shift of 3.11 ppm, (ii) the protonation state of the amine group of the glucosamine residue (Bunel et al. 1993).

GSL-B Fraction. Among the acidic GIPCs, fraction B was analyzed first because it was the most abundant; it contained only one GSL spot on HPTLC (Figure 1). The chemical shifts and coupling constants of the glycosidic moiety obtained for the GSL-B fraction are shown in Table IV. The 1D ^{1}H and 2D ^{1}H, ^{13}C gHSQC spectra exhibited three signals of equivalent areas in the anomeric region (5.029/103.85 ppm, 5.020/101.71 ppm, and 4.881/108.70 ppm) indicating the presence of three monosaccharide residues (Figure 4, Table IV). For the first two glycosidic residues, protons were assigned from the anomeric proton only up to H3 and H4 respectively using relayed COSY experiments. The missing ring protons partly located in the TOCSY experiment were fully identified using the combination of ^{1}H, ^{13}C edited HSQC and H2BC experiments recently described as a useful method for tracing the proton-bearing carbon skeleton of a molecule (Petersen et al. 2006). Sugar rings stereochemistry deduced from $^{3}J_{H,H}$ coupling constants were consistent with Manp for these two glycosidic residues. Their α-configuration was evident from $^{1}J_{C1,H1}$ coupling constant values (169.1 and 173.1 Hz). According to the GLC composition and methylation analysis (Tables I and II), the galactose residue was identified in a β-furanosic configuration by its characteristically very low field anomeric ^{13}C resonance at 108.70 ppm (Ritchie et al.

Table III. ^{1}H and ^{13}C NMR chemical shifts (ppm) and coupling constants ($J_{H,H}$ and $^{1}J_{C1H1}$, Hz) for the glycan sequence of the GSL-U fraction.
α-Manp-(1-3)-α-Manp-(1-6)-α-GlcNH$_2$-(1-2)-Ins-(1-O)-P-Cer

	H$_1$ $^{3}J_{1,2}$ C$_1$ $^{1}J_{C1H1}$	H$_2$ $^{3}J_{2,3}$ C$_2$	H$_3$ $^{3}J_{3,4}$ C$_3$	H$_4$ $^{3}J_{4,5}$ C$_4$	H$_5$ $^{3}J_{5,6}$–$^{3}J_{5,6'}$ C$_5$	H$_6$–H$_{6'}$ $^{2}J_{6,6'}$ C$_6$
α-Man-(1-3)-	4.925 *1.7* 105.26 *169.6*	3.781 *≈3* 73.56	3.606 *≈10* 74.07	3.440 *≈10* 70.57	3.468 *4.9* 76.66	3.524–3.695 *10.9* 64.41
-3)-α-Man-(1-6)-	4.666 *1.8* 103.51 *167.6*	3.932 *3.1* 72.54	3.656 *9.1* 82.24	3.576 9.7 69.06	3.468 *nm -5.0* 76.80	3.518–3.665 *12.00* 64.41
-6)-α-GlcNH2-(1-2)-	5.222 *3.5* 101.32 nm	2.923 *10.2* 57.91	3.652 *10.0* 73.83	3.320 *10.8* 72.97	3.994 *≈0 -5.2* 74.30	3.594–3.799 *11.0* 68.29
-2)-*myo*-Ins-(1-O)-P	3.825 *2.7* 79.86 $J_{H,P} = 10.4$	4.168 *2.7* 85.22	3.278 *10.0* 73.38	3.371 *8.5* 75.18	3.048 $^{3}J_{5,6} = 8.5$ 78.03	3.776 $^{3}J_{6,1} = 8.8$ 75.11

nm: not measured.

Table IV. ^{1}H and ^{13}C NMR chemical shifts (ppm) and coupling constants ($J_{H,H}$, $^{1}J_{C1H1}$, and $J_{H,P}$, Hz) for the glycan sequence of the GSL-B fraction.
β-Galf-(1-2)-α-Manp-(1-3)-α-Manp-(1-2)-Ins-(1-O)-P-Cer

	H_1 $^{3}J_{1,2}$ C_1 $^{1}J_{C1H1}$	H_2 $^{3}J_{2,3}$ C_2	H_3 $^{3}J_{3,4}$ C_3	H_4 $^{3}J_{4,5}$ C_4	H_5 $^{3}J_{5,6}$–$^{3}J_{5,6'}$ C_5	H_6–$H_{6'}$ $^{2}J_{6,6'}$ C_6
β-Galf-(1-2)-	4.881 *2.1* 108.70 *173.6*	3.788 *3.2* 83.78	3.808 *5.2* 80.10	3.936 *3.2* 87.25	3.525 *6.7–6.0* 73.90	3.377–3.401 *10.9* 65.85
-2)-α-Man-(1-3)-	5.020 *1.5* 101.71 *169.1*	3.917 *3.8* 77.08	3.607 *8.9* 72.86	3.332 *9.4* 71.05	3.584 *5.0–5.0* 76.30	3.508–3.578 *11.2* 64.00
-3)-α-Man-(1-2)-	5.029 *1.5* 103.85 *173.1*	3.927 *3.3* 72.60	3.659 *9.4* 81.70	3.608 *10.2* 68.81	3.867 *5.8–3.5* 76.16	3.488–3.561 *11.5* 64.13
-2)-*myo*-Ins-(1-O)-P	3.727 *2.4* 78.99 *139.3* $J_{H1,P} = 9.2$	3.977 *2.6* 80.91	3.216 *11.3* 73.63	3.351 *8.9* 75.29	2.948 $^{3}J_{5,6} = 8.9$ 78.56	3.485 $^{3}J_{1,6} = 9.4$ 75.49

1975). The *myo*-inositol residue was identified as previously for the GSL-U fraction. The NMR structural analysis of this fraction explicitly indicated the presence of two α-mannose, one β-galactofuranose, and one inositol residue (Table IV).

In the NOESY spectrum, the two inter-residue dipolar interactions observed between the H1 proton of the β-galactofuranose residue and the H1 and H2 protons of a mannose residue did not allow the characterization of a branching point. In the gHMBC spectrum, only H1/C2 and C1/H2 inter-residue correlations between the β-galactofuranose residue and this mannose residue were observed indicating the β-Galf-(1→2)-α-Manp motif (Figure 4). This linkage accounts for the downfield chemical shift of the mannose C2 carbon at 77.08 ppm. In the NOESY spectrum, the H1/H3 interaction between the latter mannose residue and the second mannose residue indicates a →2)-α-Manp-(1→3)-α-Manp linkage. This glycosidic sequence was confirmed by H1/C3 and C1/H3 correlations between these two mannose residues observed in the gHMBC experiments but also by the downfield chemical shift of C3 of the second mannose residue at 81.70 ppm (Table IV). The strong H1/H2 interaction between the second mannose residue and the inositol residue observed in the NOESY spectrum and the double correlation H1/C2 and C1/H2 observed in the gHMBC experiment between these two residues indicate the following sequence motif: →3)-α-Manp-(1→2)-Ins (Figure 4). This is in agreement with the downfield shift of the inositol C2 carbon resonating at 80.91 ppm (Table IV). Together with methylation and MS data (Figure 2, Table I), these NMR data established the structure of GSL-B as β-Galf-(1→2)-α-Manp-(1→3)-α-Manp-(1→2)-Ins-(1→O)-P-Cer.

GSL-A Fraction. In agreement with the TLC data, two distinct molecules were observed by NMR in the GSL-A fraction. The chemical shifts and coupling constants of the corresponding glycosidic sequences are shown in Table V. The one-dimensional ^{1}H spectrum (not shown) exhibited three signals in the anomeric region with areas in the ratio 2/1.2/2. The sugar spin systems assignment and the sequential glycosidic analysis revealed that these signals correspond to five protons belonging to two different molecules present in about equivalent amounts. The GSL-A2 molecule was identical to the GSL-B one. The GSL-A1 structure displayed the identical dimannoside core as GSL-A2 without the β-galactofuranose residue at the nonreducing end. Thus, the C2 carbon resonance of the first mannose residue was not downfield shifted for the GSL-A1 molecule (73.47 ppm) upon branching of galactofuranose as observed for the GSL-A2 molecule (77.09 ppm). Moreover, only three correlations were observed in the ^{1}H, ^{31}P HSQC (not shown) between a phosphorus atom (3.099 ppm) and the two methylene protons of the ceramide on one side (4.039 ppm and 3.658 ppm) and the H1 proton of inositol on the other side (3.738 ppm). These data are in agreement with the fact that the two molecules differ only at the nonreducing end of the glycosidic moiety. These NMR experiments indicated the presence of the following two structures: GSL A1, α-Manp-(1→3)-α-Manp-(1→2)-Ins-(1→O)-P-Cer and GSL A2, β-Galf-(1→2)-α-Manp-(1→3)-α-Manp-(1→2)-Ins-(1→O)-P-Cer.

GSL-C Fraction. In this fraction, two different molecules were also observed which differ in their glycosidic sequences (Table VI). The presence of two different molecules was also confirmed by the observation of two close sets of three correlations in the ^{1}H, ^{31}P HSQC spectrum (data not shown) corresponding to two distinct phosphorus atoms resonating at 2.478 ppm and 2.370 ppm and interacting with the two methylene protons of the ceramide ($\delta = 4.002 - 3.667$ ppm and $\delta = 3.997 - 3.670$ ppm respectively) and the H1 proton of *myo*-inositol at 3.720 ppm and 3.713 ppm, respectively. The one-dimensional ^{1}H-NMR spectrum (not shown) exhibited eight H1 resonances of about equal intensity. In the anomeric region of the 2D ^{1}H, ^{13}C gHSQC spectrum (not shown), six resonances among the eight were grouped two by two that resembled the anomeric region of the GSL-B fraction. Indeed, the sugar spin systems assignment and the sequential glycosidic

Table V. ^{1}H and ^{13}C NMR chemical shifts (ppm) and coupling constants ($J_{H,H}$ and $^{1}J_{C1H1}$, Hz) for the two glycan sequences of the GSL-A fraction. GSL-A1: α-Manp-(1-3)-α-Manp-(1-2)-Ins(1-O)-P-Cer GSL-A2: β-Galf- (1-2)-α-Manp-(1-3)-α-Manp-(1-2)-Ins(1-O)-P-Cer.

	H_1 $^{3}J_{1,2}$ C_1 $^{1}J_{C1H1}$	H_2 $^{3}J_{2,3}$ C_2	H_3 $^{3}J_{3,4}$ C_3	H_4 $^{3}J_{4,5}$ C_4	H_5 $^{3}J_{5,6}$–$^{3}J_{5,6'}$ C_5	H_6–$H_{6'}$ C_6
GSL-A1						
α-Manp-(1-3)-	4.905	3.733	3.586	3.446	3.605	3.51–3.58
	2.2	*4.2*	*9.4*	*8.8*	3.595[a]	3.53[a]–3.60[a]
	104.67	73.47	74.00	70.55	76.38	64.14
	170.0				76.42[a]	64.05[a]
-3)-α-Manp-(1-2)-	5.044	3.932	3.641	3.638	3.889	3.51–3.58
	1.7	*4.5*		*10.2*	*6.6*	
	103.88	72.63	81.5	68.85	76.18	64.14
	173.4					
-2)-*myo*-Ins-(1-O)-P	3.738	3.977	3.227	3.369	2.953	3.501
	3.5	*3.4*	*9.8*	*9.6*	*9.6*	$^{3}J_{6,1} \approx 9.5$
	78.94	80.91	73.66	75.24	78.68	75.50
GSL-A2						
β-Galf- (1-2)-	4.901	3.808	3.821	3.956	3.540	3.401–3.422
	1.8	*4.6*	*4.0*	*4.5*		
	108.72	83.79	80.06	87.27	73.90	65.84
	173.8					
-2)-α-Manp-(1-3)-	5.035	3.935	3.624	3.364	3.605	3.53–3.60
	1.6	*4.0*	*9.4*	*9.5*	3.595[a]	
	101.66	77.09	72.86	71.13	76.38	64.05
	169.2				76.42[a]	
-3)-α-Manp-(1-2)-	5.044	3.951	3.665	3.638	3.889	3.51–3.58
	1.7	*4.5*	*10.2*	*10.2*	*6.6*	
	103.88	72.59	81.85	68.85	76.18	64.14
	173.4					
-2)-*myo*-Ins-(1-O)-P	3.738	3.977	3.227	3.369	2.953	3.501
	3.5	*3.4*	*9.8*	*9.6*	*9.6*	$^{3}J_{6,1} \approx 9.5$
	78.94	80.91	73.66	75.24	78.68	75.50

[a]Possible chemical shift.

analysis corresponded to the same glycosidic sequence which is β-Galf-(1→2)-α-Manp-(1→3)-α-Manp-(1→2)-Ins. One of the other anomeric signals at 4.799/111.10 ppm corresponded to a second β-galactofuranose residue identified by its characteristic downfield shifted anomeric carbon. The last anomeric signal at 4.640/102.57 ppm was assigned to an α-mannopyranose residue. The ^{1}H, ^{13}C edited gHSQC methylene region of the GSL-C fraction compared to that of the GSL-B fraction showed two extra downfield shifted C6 at 68.27 ppm and 69.79 ppm indicating that the two corresponding mannose residues were 6-*O*-substituted.

Thus, NMR data allowed the identification of the two following molecules:

GSL-C1, β-Galf(1→2)-α-Manp(1→3)-[α-Manp(1→6)]-α-Manp-(1→2)-Ins(1→O)-P-Cer and GSL-C2, β-Galf(1→2)-α-Manp(1→3)-[β-Galf(1→6)]-α-Manp-(1→2)-Ins(1→O)-P-Cer.

GSL-D Fraction. The chemical shifts and coupling constants obtained for this fraction are summarized in Table VII. The 1D ^{1}H and 2D ^{1}H, ^{13}C gHSQC spectra exhibited three signals of equivalent areas in the anomeric region (5.108/103.47 ppm, 5.069/102.24 ppm, and 4.939/109.11 ppm), indicating the presence of three monosaccharides (Figure 5). The glycosidic ring spin systems assignment and coupling constants examination permitted the identification of two α-mannose residues and one β-galactofuranose residue as in the GSL-B fraction. Moreover, the NOESY and gHMBC spectra showed the same inter-residue connectivities as those observed for the GSL-B fraction (Figures 4 and 5), emphasizing the monosaccharide sequence identity with GSL-B. However, differences were observed when comparing ^{1}H, ^{13}C HSQC spectra of the two fractions (Figures 4 and 5). Thus, a large downfield shift at 68.92 ppm and a smaller upfield shift at 72.11 ppm were observed for the C6 and C5 carbons respectively of the β-Galf residue for the GSL-D fraction, indicating a 6-*O* substitution for this residue. Furthermore, in a gHSQC experiment, two new methylene carbons and one trimethyl group have been identified at 4.127/61.62 ppm, 3.571/68.79 ppm, and 3.169/56.48 ppm respectively. The COSY experiment showed that these methylene carbons were linked together. The characteristic methyl ^{13}C shift is consistent with the MS data (Figure 2), indicating the presence of an *N*-trimethyl group (Figure 5). In the HMBC spectrum, two ^{1}H, ^{13}C long-range interactions were observed between this *N*-trimethyl group and the second methylene group indicating the presence of the $(CH_3)_3$–N–CH_2–CH_2 motif. Two sets of correlations were observed in the ^{1}H, ^{31}P HSQC (Figure 5). A first set of three correlations was detected between a phosphorus atom (2.974 ppm) and the two methylene protons of the ceramide on one side (4.094 ppm and 3.660 ppm) and the H1 proton of inositol on the other side (3.756 ppm), corresponding to the IPC. Another set of two correlations was observed between a second phosphorus atom (0.763 ppm) and the two extra methylene protons on the one hand (4.127 ppm) and the H6 protons of β-Galf on the other hand (3.764 ppm). This was in agreement

Table VI. ^{1}H and ^{13}C NMR chemical shifts (ppm) and coupling constants ($J_{H,H}$ and $^{1}J_{C1H1}$, Hz) for the two glycan sequences of the GSL-C fraction. GSL-C1: β-Galf(1-2)-α-Manp(1-3)-[α-Manp (1-6)]-α-Manp-(1-2)- Ins(1-O)-P-Cer GSL-C2: β-Galf(1-2)-α-Manp(1-3)-[β-Galf (1-6)]-α-Manp-(1-2)- Ins(1-O)-P-Cer.

	H_1 $^{3}J_{1,2}$ C_1 $^{1}J_{C1H1}$	H_2 $^{3}J_{2,3}$ C_2	H_3 $^{3}J_{3,4}$ C_3	H_4 $^{3}J_{4,5}$ C_4	H_5 $^{3}J_{5,6}$–$^{3}J_{5,6'}$ C_5	H_6–$H_{6'}$ C_6
GSL-C1						
β-Galf- (1-2)-	4.877	3.777	3.800	3.933	3.518	3.360–3.392
	1.1	*2.9*				
	108.47	83.60	79.93	87.07	73.72	65.72
	174.7					
-2)-α-Manp-(1-3)-	4.989	3.933	3.604	3.325	3.565	3.507–3.599
	3.2	*3.5*				3.451[a]–3.595[a]
	101.72	76.81	72.77	70.79	76.29	63.74
	169.3					64.17[a]
α-Manp-(1-6)-	4.640	3.642	3.506	3.366	3.380	3.445–3.602
	1.5–2.5	*3.1*				
	102.57	73.20	73.72	70.07	76.51	64.17
	169.1					
-3,6)-α-Manp-(1-2)-	4.982	3.924	3.621	3.632	4.021	3.486–3.702
	3.2	*2.5*				
	103.83	72.43	82.02	68.27	74.31	68.27
	174.6					
-2)-*myo*-Ins-(1-O)-P	3.706	3.949	3.208	3.337	2.936	3.480
	Weak	*4.8*	*8.5*	*9.0*	$^{3}J_{5,6} = 8.8$	$^{3}J_{6,1} = 9.4$
	78.92	80.70	73.43	75.15	78.49	75.42
GSL-C2						
β-Galf-(1-2)-	4.877	3.777	3.800	3.933	3.518	3.360–3.392
	1.1	*2.9*				
	108.47	83.60	79.93	87.07	73.72	65.72
	174.7					
-2)-α-Manp-(1-3)-	5.003	3.916	3.594	3.325	3.565	3.507–3.599
	2.5	*3.4*				3.451[a]–3.595[a]
	101.63	76.81	72.77	70.79	76.29	63.74
	169.3					64.17[a]
β-Galf-(1-6)-	4.799	3.806	3.779	3.759	3.486	3.507–3.599
	1.9–2.5	*3.7*				3.451[a]–3.595[a]
	111.1	84.25	79.87	85.71	73.78	63.74
	171.3					64.17[a]
-3,6)-α-Manp-(1-2)-	4.982	3.921	3.643	3.581	4.013	3.429–3.747
	2.6	*2.9*	*10.2*	*10.2*	*6.6*	
	103.83	72.43	81.58	68.87	74.97	69.79
	174.6					
-2)-*myo*-Ins-(1-O)-P	3.699	3.967	3.203	3.337	2.936	3.468
	Weak	*4.8*	*8.5*	*9.0*	$^{3}J_{5,6} = 8.8$	$^{3}J_{6,1} = 9.4$
	78.93	81.13	73.43	75.15	78.49	75.42

[a]Possible chemical shift.

with the chemical shifts observed for C6 and C5 carbons resonances of the β-Galf residue, indicating its substitution by a phosphocholine residue. In addition, the comparison with the ^{1}H 1D and ^{1}H, ^{13}C HSQC spectra of a phosphatidylcholine reference compound (Sigma, St. Louis, MO) confirmed the resonances assignment of the phosphocholine (not shown). Thus, the NMR analysis, in agreement with methanolysis/trimethylsylation, methylation, and MS data, showed that the GSL-D fraction corresponded to Cho-P-(O→6)-β-Galf-(1→2)-α-Manp-(1→3)-α-Manp-(1→2)-Ins(1→O)-P-Cer. The substitution of galactofuranose residue by a phosphate group explains the low amount of galactose detected by GLC (Table I).

Discussion

The results presented here and in previous studies show that *A. fumigatus* produced at least nine GIPCs of different structures (Table VIII). All GSLs have the same ceramide moiety composed of a 2-hydroxylated lignoceric acid (2-OH $C_{24:0}$) associated with a $C_{18:0}$-phytosphingosine base. This lipid moiety is common to most fungi species. The glycan part has more variability and two types of GIPCs have been isolated from *A. fumigatus* mycelium. First, a zwitterionic GSL that is the major GIPC from *A. fumigatus* mycelium contains a glucosamine residue linked in α1-2 to the inositol ring. This unusual carbohydrate sequence has been recently described in *A. fumigatus* by Toledo et al. (2007) and has been described in only two other fungal pathogens, *S. schenckii and Acremonium sp*. (Toledo, Levery, Glushka et al. 2001; Aoki, Uchiyama, Itonori et al. 2004). Secondly, the five other acidic GSL structures contain a common sequence α-Man-(1-3)-α-Man-(1-2)-Inositol. This sequence has been previously described in *A. fumigatus* GSL (Levery et al. 2001; Toledo et al. 2007) and other fungal species (Levery et al. 1998, 2001; Bennion et al. 2003; Barr and Lester 1984). No α-Man-(1-6)-Inositol as found in *S. schenckii* (Toledo, Levery, Glushka et al. 2001; Loureiro y Penha et al. 2001) and no

Table VII. ^{1}H, ^{13}C, and ^{31}P NMR chemical shifts (ppm) and coupling constants ($J_{H,H}$, $^{1}J_{C1H1}$, and $J_{H,P}$, Hz) for the glycan sequence and for the phosphocholine sequence of the GSL-D fraction. Cho-P-(O-6)-β-Galf-(1-2)-α-Manp-(1-3)-α-Manp-(1-2)-Ins(1-O)-P-Cer.

Glycan moiety	H_1 $^{3}J_{1,2}$ C_1 P	H_2 $^{3}J_{2,3}$ C_2	H_3 $^{3}J_{3,4}$ C_3	H_4 $^{3}J_{4,5}$ C_4	H_5 $^{3}J_{5,6}$–$^{3}J_{5,6'}$ C_5	H_6–$H_{6'}$ C_6 P
P-(O-6)-β-Galf-(1-2)-	4.939 *1,8* 109.11	3.894 83.74	3.898 79.46	3.974 86.66	3.696 72.11	3.764 68.92 0.763 $J_{H1,P} = 7.5$
-2)-α-Manp-(1-3)-	5.069 *1.6* 102.24	3.964 *5.2* 77.25	3.672 *9.6* 73.19	3.413 *9.6* 71.07	3.643 76.70	3.651–3.562 64.14
-3)-α-Man-(1-2)-	5.108 *1.9* 103.47	3.959 *4.7* 72.66	3.745 82.26	3.647 68.87	3.958 76.22	3.566 64.29
-2)-*myo*-Ins-(1-O)-P	3.756 *2.4* 79.07 2.974 $J_{H1,P} = 8.6$	3.982 *2.5* 80.43	3.237 *9.4* 74.07	3.433 *9.1* 75.25	2.973 $^{3}J_{5,6} = 9.1$ 79.00	3.538 $^{3}J_{1,6} = 9.2$ 75.74
Choline–phosphate substitution	 ^{1}H ^{13}C ^{31}P					
CH_2OP	4.127 61.62 0.763					
CH_2N	3.571 68.79					
$N(CH_3)_3$	3.169 56.48					

α-Man-(1-4)-inositol as found in mushrooms (Jennemann et al. 1999) have been observed in *A. fumigatus* GSLs. Four of the five acidic GSLs analyzed contained galactofuranose in *A. fumigatus*. The presence of galactofuranose in GSLs has been reported in human pathogens such as *Histoplasma capsulatum, Paracoccidioïdes brasiliensis, A. fumigatus* (Barr and Lester 1984; Levery et al. 1998; Toledo et al. 2007). In these later structures, the galactofuranose residue is linked to the first mannose as for the GSL-C2 of *A. fumigatus*. However, the galactofuranose residue is mainly linked to the terminal nonreduced mannose residue through a β1-2 linkage (GSL-B). Surprisingly, a choline–phosphate group has been localized to the terminal galactofuranose residue (GSL-D). A choline–phosphate in a GSL structure has also been found in *Acremonium sp*.; however, it is linked to a mannose residue instead of a galactofuranose residue (Aoki, Uchiyama, Itonori et al. 2004). Some discrepancies are seen between our data and the study of Toledo et al. (2007). These authors did not observe the β-galactofuranose linked in β1-2 to the terminal mannose and the choline–phosphate linked to this β-galactofuranose. In contrast, they described the presence of a mannose residue linked in α1-2 to Man_2-IPC that we did not observe. These differences are not explained and could be due to the use of different growth conditions or to different strains.

GIPCs have been mainly analyzed in human fungal pathogens (*A. niger, H. capsulatum, P. brasiliensis, S. schenckii,* and *C. neoformans*), and it has been suggested that GIPCs have an immunological function during fungal infection. The presence of galactofuranose in these GIPCs that is absent in mammals seems to play an important role in fungal–host interactions. Earlier studies have shown that galactofuranose containing molecules of *A. fumigatus* are extremely antigenic (Latgé et al.

Table VIII. GIPC structures described in *Aspergillus fumigatus*

Structures of GIPC	References
α-Man-(1-3)-α-Man-(1-6)-α-GlcN-(1-2)-Ins-P-cer	Toledo et al. 2007; this study
α-Man-(1-3)-α-Man-(1-2)-Ins-P-cer	Levery et al. 2001; Toledo et al. 2007; this study
α-Man-(1-2)-α-Man-(1-3)-α-Man-(1-2)-Ins-P-cer	Toledo et al. 2007
α-Man-(1-3)-[β-Galf-(1-6)]-α-Man-(1-2)-Ins-P-cer	Toledo et al. 2007
α-Man-(1-2)-α-Man-(1-3)-[β-Galf-(1-6)]-α-Man-(1-2)-Ins-P-cer	Toledo et al. 2007
β-Galf-(1-2)-α-Man-(1-3)-α-Man-(1-2)-Ins-P-cer	This study
β-Galf-(1-2)-α-Man-(1-3)-[α-Man-(1-6)]-α-Man-(1-2)-Ins-P-cer	This study
β-Galf-(1-2)-α-Man-(1-3)-[β-Galf-(1-6)]-α-Man-(1-2)-Ins-P-cer	This study
Choline-P-6-β-Galf-(1-2)-α-Man-(1-3)-α-Man-(1-2)-Ins-P-cer	This study

1994; Costachel et al. 2005; Morelle et al. 2005; Leitao et al. 2003). Galactofuranose residues are also an immunodominant in GSLs of *P. brasiliensis* and *H. capsulatum* (Barr and Lester 1984; Levery et al. 1998). In *Leishmania major*, a monoclonal antibody against a glycolipid containing terminal galactofuranose residue can reduce the macrophage infectivity of this parasite (Suzuki et al. 2002). The expression in infected human tissues of intelectin that recognizes a single terminal galactofuranose residue (Tsuji et al. 2001) is in agreement with the involvement of galactofuranosylated GSLs during infection. Antibodies from patients with aspergillosis recognized the *A. fumigatus* GIPCs isolated by Toledo et al. (2007); however, the role of *A. fumigatus* GIPCs in host cellular immunity has not been defined as yet.

The biosynthetic pathway of sphingolipids begins in the endoplasmic reticulum where it proceeds to the formation of the ceramide moiety. A linkage between the carbohydrate and phytosphingosine occurs in the Golgi apparatus (Funato et al. 2002; Dickson et al. 2006). In yeast, ceramide biosynthesis and inositol addition are essential for growth. Indeed, GIPCs are involved in cell regulation, cell polarity, stress response, trafficking, and cell wall integrity (Dickson et al. 2006). Similarly, in *Aspergillus*, the gene encoding the IPC synthase is essential for fungal growth as well as basA gene encoding a phytosphingosine (Li et al. 2007). Sphingolipids are involved in polarized growth via the control of actin cytoskeleton (Cheng et al. 2001; Hu et al. 2007). This result is in agreement with the susceptibility of *Aspergillus* species to various inhibitors of a sphingolipid synthesis pathway (Zhong et al. 2000; Li et al. 2007). In *A. fumigatus*, three types of membrane-anchored molecules present the same IPC lipid moiety: GPI-anchored protein (Fontaine et al. 2003), the lipogalactomannan, a GPI-anchored polysaccharide (Costachel et al. 2005), and GIPCs. In this study, the inositol ring of an IPC structure could be substituted in position 2 by a mannose or a glucosamine residue. In contrast, previous studies suggested that the glucosamine residue is linked in α1-6 to the inositol ring in the GPI-anchor structures from GPI-protein or from the lipogalactomannan.

In *S. cerevisiae*, two homologous genes of IPC mannosyltransferases are involved in the addition of the first mannose residue to the inositol ring. The deletion of both genes is not lethal, but mutants are sensitive to the external Ca^{2+} (Beeler et al. 1997), suggesting a role for the GSLs in cellular stress response. In *C. albicans*, the deletion of the MIT1, an IPC mannosyltransferase homologue induced the absence of MIPC, M(IP)2C and the phospholipomannan (β1-2mannan linked to MIPC) and decreased virulence of the mutant (Trinel et al. 2002; Mille et al. 2004). In *A. fumigatus*, no such mutant has been described, so the relevance of these GIPCs during *A. fumigatus* growth and host–pathogen interactions is still unknown.

Materials and methods

Fungal culture and membrane preparation

A. fumigatus, strain CBS 144–89 was grown in a 15-L fermenter in 2% glucose and 1% mycopeptone (Biokar Diagnostics, Pantin, France) for 24 h at 25°C as described previously (Hartland et al. 1996). The mycelium was collected by filtration under vacuum, washed with water, and then disrupted in 200 mM Tris–HCl, 20 mM EDTA, pH 8.0, 1 mM PMSF buffer at 4°C with glass beads (1 mm, diameter) in a Dyno mill apparatus (W. A. Bachofen AG, Basel, Switzerland). The cell wall was removed by centrifugation at 10,000 × *g* 10 min at 4°C. Total membranes were then collected by ultracentrifugation at 125,000 × *g* 60 min at 4°C. Membrane pellet was homogenized in the disruption buffer with a Dounce homogenizer and then centrifuged once more at 125,000 × *g* for 60 min at 4°C. Pellet was resuspended again in 20 mM Tris–HCl, 2 mM EDTA, pH 8.0 and store at −80°C.

Extraction and purification of glycosylinositolphosphatidylceramides

A chloroform/methanol mixture was added to the membrane suspension (20 mg of protein/mL) to obtain a chloroform/methanol/membrane ratio of 10/10/3 respectively. The mixture was stirred for 2 h at room temperature, and then centrifuged at 10,000 × *g* for 10 min. The pellet was resuspended in a chloroform/methanol/water (10/10/3, v/v/v) mixture, and the extraction was repeated once. Pooled supernatants were concentrated under vacuum with a rotavapor, and the residue was submitted to a butanol/water partition. The water phase containing GIPCs was dialyzed against water and freeze-dried. The residue was dissolved in chloroform/methanol/water (10/15/4, v/v/v) and applied onto a DEAE-Sephadex A-25 column (GE Healthcare Bio-Sciences, Uppsala, Sweden, 2 × 15 cm) equilibrated in the same solvent at the flow rate of 30 mL/h. Unbound products were eluted with 2 column volumes of solvent, and then retained products were eluted by a chloroform/methanol/NH_4Ac 1 M (10/15/4) solvent. Carbohydrates were detected by spraying with orcinol sulfuric acid on spot of 2 μL of different fractions on silica sheets. Fractions containing sugars were concentrated and then dialyzed against water and freeze-dried. GIPCs were then purified on a silica 60 column (Merck, Darmstadt, Germany 1.8 × 30 cm), equilibrated in propanol-1/water/NH_4OH 30% (85/15/5, v/v/v) and eluted at 25 mL/h. Samples were deposited onto the silica 60 column and eluted by 3 column volumes of propanol-1/water/NH_4OH 30% (85/15/5, v/v/v), then 3 volumes of propanol-1/water/NH_4OH 30% (80/20/5, v/v/v), and then 3 volumes of propanol-1/water/NH_4OH 30% (70/30/5, v/v/v). The presence of carbohydrate in the fraction was detected as described above. Fractions were dialyzed against water and freeze-dried.

Analytical methods

Neutral hexoses were identified by GLC as alditol acetates obtained after hydrolysis (4 N trifluoroacetic acid, 100°C, 4 h) (Sawardeker et al. 1967). Glucosamine and *myo*-inositol were quantified by GLC-MS after hydrolysis (6 N HCL, 110°C 20 h), N-acetylation and trimethysilyation, using the *scyllo*-inositol as a standard (Ferguson 1993). Lipid analysis was performed by GLC-MS on HF-treated GIPC fraction (aqueous 50% HF, 2 days on ice). Fatty acids and sphingosine bases were released by methanolysis (1 N HCl in MeOH, 80°C, 20 h). Fatty acids were extracted with heptane and analyzed after trimethylsilylation. The methanol phase containing the sphingosine base was N-acetylated, trimethylsilylated, and analyzed by GLC-MS. Phosphorylated carbohydrates were identified by GLC-MS after acid methanolysis (1 N HCL in methanol, 80°C, 20 h) and trimethylsilylation (Ferguson 1993). The lipophosphoglycan from *L. donovani,* a kind gift from Pascale Pescher (Unité

de Virulence Parasitaire, Institut Pasteur), was used as a positive control. Methylation of GSL fractions was performed using the sodium hydroxide procedure (Ciucanu and Kerek 1984). GSL containing a glucosamine residue was peracetylated with a pyridine/acetic anhydride solution (50/200 μL) overnight at room temperature prior to the methylation procedure. Methyl ethers were analyzed by GLC-MS as polyolacetates (Björndal et al. 1970).

HPTLC. GIPC fractions were applied to a 10-cm aluminum-backed silica gel 60 (Merck) and developed with chloroform/methanol/1 M ammonium acetate/NH_4OH 30%/water (180/140/9/9/23). Sugars were detected with orcinol-sulfuric acid.

GLC and GLC Mass Spectrometry. GLC was performed on a Delsi 200 instrument with a flame ionization detector using a capillary column (30 m × 0.25 mm id) filled with a EC^{TM}-1 (Alltech, Templemars, France) under the following conditions: gas vector and pressure, helium 0.7 bar; temperature program 120 to 180°C at 2°C/min and 180 to 240°C at 4°C/min. GLC-MS was performed on an Automass II apparatus (Finigan, Thermo Electron Corporation, Runcorn, UK) coupled to a CarloErba gas chromatograph (model 8000 top), using a capillary column (30 m × 0.25 mm id) filled with a EC^{TM}-1 (Alltech) under the following conditions: gas vector and flow rate, helium 1.2 mL/min; temperature program for inositol and monosaccharide analysis: 100 to 200°C at 5°C/min, 200 to 240°C at 15°C/min, and 240°C for 5 min; temperature program for sphingosine base and fatty acid analysis: 100 to 200°C at 10°C/min, 200 to 260°C at 15°C/min, and 260°C for 13 min.

Nanoelectrospray mass spectrometry. Mass spectrometric analyses were performed in the negative mode using a Q-STAR Pulsar quadrupole time-of-flight (Q-TOF) mass spectrometer (AB/MDS Sciex, Toronto, Canada) equipped with a nanoelectrospray ion source (Protana, Odense, Denmark).

The samples in propanol-1/H_2O (25/75) dissolved in chloroform/methanol (50/50) were sprayed from gold-coated "medium length" borosilicate capillaries (Protana). A potential of −800 V was applied to the capillary tip. The declustering potential was set at −120 V and the focusing potential was set at −200 V. The molecular ions were then selected in the quadrupole analyzer and partially fragmented in the hexapole collision cell, with the pressure of collision gas (N_2) 5.3×10^{-5} Torr (1 Torr = 133.3 Pa). The collision energy varied between −40 and −80 eV depending on the sample. For the recording of conventional mass spectra, TOF data were acquired by accumulation of 10 multiple channel acquisition (MCA) scans over mass ranges of *m*/*z* 500–1800 Daltons for MS analyses and over mass ranges of *m*/*z* 50–1800 for MS/MS analyses. Data acquisition was optimized to supply the highest possible resolution and the best signal-to-noise ratio, even in the case of low abundance signals. Typically, the full width at half maximum (FWHM) was 7000 in the measured mass ranges. External calibration was performed prior to each measure using a 4 pmol/μL solution of taurocholic acid in acetonitrile/water (50/50, v/v) containing 2 mM of ammonium acetate.

NMR Spectroscopy. NMR spectra were acquired at 50°C on a Varian, Les Ulis, France Inova 500 spectrometer equipped with a triple $^1H\{^{13}C/^{15}N\}$ resonance ^1H PFG probe or an indirect PFG probe for ^1H, ^{31}P experiments. For the low-concentration samples, complementary experiments were performed at 35°C on a Varian Inova 600 spectrometer equipped with a cryogenically cooled triple resonance $^1H\{^{13}C/^{15}N\}$ PFG probe. Samples were dissolved in DMSO-d6 for NMR (99.96% ^2H atoms, Euriso-top, CEA, Saclay, France) and transferred in 5 mm Shigemi tubes (Shigemi Inc., Allison Park, PA). D_2O (99.97% 2H atoms, Euriso-top) was added in order to exchange sugars hydroxyl protons. Since the proton chemical shift of the residual signal of DMSO-d6 depends on temperature and water content, external referencing was applied for ^1H chemical shifts using a capillary containing a freshly prepared solution of 20 mM DSS in DMSO-d6 containing less than 0.01% of water. The DSS methyl resonance was set to 0 ppm. ^{13}C chemical shifts were then calculated from the ^1H chemical shift and gamma ratio relative to DSS. The $^{13}C/^1H$ gamma ratio of 0.251449530 was used (Wishart et al. 1995). ^{31}P chemical shifts were determined with neat phosphoric acid (Wilmad-Labglas, NJ) by the substitution method.

For all GSL fractions, the same general strategy was adopted for assignment of nuclei. First, the proton resonances were assigned using two-dimensional COSY and RELAY experiments with one to three relays to follow connectivities from the anomeric proton up to the H5 proton of most of the glycosidic residues (Rance et al. 1983; Wagner 1983). The intraglycosidic residue spin systems were often completed by mean of a TOCSY experiment with a long mixing time (120 ms) (Griesinger et al. 1988). A ^1H–^{13}C edited gHSQC experiment allowed to achieve ^{13}C chemical shifts assignment from previously identified ^1H resonances (Willker et al. 1993). Then, ^1H, ^1H coupling constants analysis from the 1D and/or COSY spectrum (^1H resolution of 0.1 Hz and 1.6Hz respectively) was used to assess the identity of monosaccharide residues. Moreover, the anomeric configuration of monosaccharide residues was established from knowledge of $^3J_{1,2}$ values and confirmed by the measurement of the $^1J_{C1H1}$ heteronuclear coupling constants in the ^1H dimension of the undercoupled gHSQC spectrum (^1H resolution of 0.6 Hz) or of the gHMBC spectrum (^1H resolution of 1.2 Hz) (Willker et al. 1993). Finally, glycosidic linkages were established via through-space dipolar interactions using a ^1H–^1H NOESY experiment (mixing time of 200 ms) (Macura et al. 1981) and/or via three-bond interglycosidic ^1H–^{13}C correlations using a ^1H–^{13}C gHMBC experiment (long-range delay of 60 ms). In addition, the branching point between the phospholipid and the glycosidic moieties was identified using the ^1H–^{31}P gHSQC.

Acknowledgement

We thank Professor R. Calderone (Georgetown University Medical center, Washington) for reading of the manuscript.

Conflict of interest statement

None declared.

Abbreviations

COSY, correlation spectroscopy; DMSO, dimethylsulfoxyde; DSS, 2,2-dimethyl-2-silapentane-5-sulfonate sodium salt; FWHM, full width at half maximum; gHMBC, gradient selected

heteronuclear multiple bond correlation; gHSQC, gradient selected heteronuclear single-quantum correlation; GIPC, glycosylinositolphosphoceramide; GLC, gas–liquid chromatography; GLC-MS: gas–liquid chromatography mass spectrometry; GPI, glycosylphosphatidylinositol; GSL, glycosphingolipid; H2BC, heteronuclear two-bond correlation; HPTLC, high-performance thin layer chromatography; IPC, inositolphosphoceramide; MCA, multiple channel acquisition; MS, mass spectrometry; NMR, nuclear magnetic resonance; NOESY, nuclear Overhauser effect spectroscopy; PFG, pulsed field gradient; Q-TOF, pulsar quadrupole-time of flight; RELAY 2D, relayed COSY; TOCSY, total correlation spectroscopy.

References

Aoki K, Uchiyama R, Itonori S, Sugita M, Che FS, Isogai A, Hada N, Hada J, Takeda T, Kumagai H et al. 2004. Structural elucidation of novel phosphocholine-containing glycosylinositol-phosphoceramides in filamentous fungi and their induction of cell death of cultured rice cells. Biochem J. 378:461–472.

Aoki K, Uchiyama R, Yamauchi S, Katayama T, Itomori S, Sugita M, Hada N, Yamada-Hada J, Takeda T, Kumagai H et al. 2004. Newly discovered neutral glycosphingolipids in aureobasidin A-resistant *Zygomycetes*. J Biol Chem. 279:32028–32034.

Arigi E, Singh S, Kahlili AH, Winter HC, Goldstein IJ, Levery SB. 2007. Characterization of neutral and acidic glycosphingolipids from the lectin-producing mushroom, *Polyporus squamosus*. Glycobiology. 17:754–766.

Barr K, Laine RA, Lester RL. 1984. Carbohydrate structures of three novel phosphoinositol-containing sphingolipids from the yeast *Histoplasma capsulatum*. Biochemistry. 23:5589–5596.

Barr K, Lester RL. 1984. Occurrence of novel antigenic phosphoinositol-containing sphingolipids in the pathogenic yeast *Histoplasma capsulatum*. Biochemistry. 23:5581–5588.

Barreto-Bergter E, Pinto MR, Rodrigues ML. 2004. Structure and biological functions of fungal cerebrosides. An. Acad. Bras. Cienc. 76:67–84.

Beeler TJ, Fu D, Rivera J, Monaghan E, Gable K, Dunn TM. 1997. *SUR1 (CSG1/BCL21)*, a gene necessary for growth of *Saccharomyces cerevisiae* in the presence of high Ca^{2+} concentrations at 37°C, is required for mannosylation of inositolphosphorylceramide. Mol Gen Genet. 255:570–579.

Bennion B, Park C, Fuller M, Lindsey R, Momany M, Jennemann R, Levery SB. 2003. Glycosphingolipids of the model fungus *Aspergillus nidulans*: Characterization of GIPCs with oligo-alpha-mannose-type glycans. J Lipid Res. 44:2073–2088.

Björndal H, Hellerqvist CG, Lindberg B, Svensson S. 1970. Gas-liquid chromatography and mass spectrometry in methylation analysis of polysaccharides. Angew Chem Int. 9:610–619.

Bock K, Pedersen C. 1974. A study of ^{13}CH coupling constants in hexopyranoses. J Chem Soc Perkin Trans. II:293–297.

Bock K, Pedersen C. 1983. Carbon-13 nuclear magnetic resonance spectroscopy of monosaccharides. Adv Carbohydr Chem Biochem. 41:27–44.

Bunel S, Ibarra C, Moraga E, Blasko A, Bunton CA. 1993. Structures of complexes of cobalt (III) and glucosamine. Applications of molecular mechanics and NMR spectroscopy. Carbohydr Res. 244:1–14.

Cheng J, Park TS, Fischl AS, Ye XS. 2001. Cell cycle progression and cell polarity require sphingolipid biosynthesis in *Aspergillus nidulans*. Mol Cell Biol. 21:6198–6209.

Ciucanu I, Kerek F. 1984. A simple and rapid method for the permethylation of carbohydrates. Carbohydr Res. 131:209–217.

Costachel C, Coddeville B, Latgé JP, Fontaine T. 2005. Glycosylphosphatidylinositol-anchored fungal polysaccharide in *Aspergillus fumigatus*. J Biol Chem. 280:39835–39842.

da Silva AF, Rodrigues ML, Farias SE, Almeida IC, Pinto MR, Barreto-Bergter E. 2004. Glucosylceramides in *Colletotrichum gloeosporioides* are involved in the differentiation of conidia into mycelial cells. FEBS Lett. 561:137–143.

Dickson RC, Sumanasekera C, Lester RL. 2006. Functions and metabolism of sphingolipids in *Saccharomyces cerevisiae*. Prog Lipid Res. 45:447–465.

Ferguson MAJ. 1993. GPI-Membrane Anchors: Isolation and Analysis in Glycobiology, A Practical Approach. Fukuda M, Kobata A, editors. Oxford, UK: Oxford University, IRL Press. pp. 349–383.

Fontaine T, Magnin T, Melhert A, Lamont D, Latgé JP, Ferguson MA. 2003. Structures of the glycosylphosphatidylinositol membrane anchors from *Aspergillus fumigatus* membrane proteins. Glycobiology. 13:169–177.

Funato K, Vallee B, Riezman H. 2002. Biosynthesis and trafficking of sphingolipids in the yeast *Saccharomyces cerevisiae*. Biochemistry. 41:15105–15114.

Griesinger C, Otting G, Wüthrich K, Ernst RR. 1988. Clean TOCSY for proton spin system identification in macromolecules. J Am Chem Soc. 110:7870–7872.

Gutierrez ALS, Farage L, Melo MN, Mohana-Borges RS, Guerardel Y, Coddeville B, Wieruszeski J-M, Mendonça-Previato L, Previato JO. 2007. Characterization of glycoinositolphosphoryl ceramide structure mutant strains of *Cryptococcus neoformans*. Glycobiology. 17:1C–11C.

Hartland RP, Fontaine T, Debeaupuis JP, Simenel C, Delepierre M, Latgé JP. 1996. A novel beta-(1-3)-glucanosyltransferase from the cell wall of *Aspergillus fumigatus*. J Biol Chem. 271:26843–26849.

Heise N, Gutierrez AL, Mattos KA, Jones C, Wait R, Previato JO, Mendonca-Previato L. 2002. Molecular analysis of a novel family of complex glycoinositolphosphoryl ceramides from *Cryptococcus neoformans*: Structural differences between encapsulated and acapsular yeast forms. Glycobiology. 12:409–420.

Hu W, Sillaots S, Lemieux S, Davison J, Kauffman S, Breton A, Linteau A, Xin C, Bowman J, Becker J et al. 2007. Essential gene identification and drug target prioritization in *Aspergillus fumigatus*. PLoS Pathog. 3:e24.

Jennemann R, Bauer BL, Bertalanffy H, Geyer R, Gschwind RM, Selmer T, Wiegandt H. 1999. Novel glycoinositolphosphosphingolipids, basidiolipids, from *Agaricus*. Eur J Biochem. 259:331–338.

Jennemann R, Geyer R, Sandhoff R, Gschwind RM, Levery SB, Grone HJ, Wiegandt H. 2001. Glycoinositolphosphosphingolipids (basidiolipids) of higher mushrooms. Eur J Biochem. 268:1190–1205.

Latgé JP. 1999. *Aspergillus fumigatus* and aspergillosis. Clin Microbiol Rev. 12:310–350.

Latgé JP, Kobayashi H, Debeaupuis JP, Diaquin M, Sarfati J, Wieruszeski JM, Parra E, Bouchara JP, Fournet B. 1994. Chemical and immunological characterization of the extracellular galactomannan of *Aspergillus fumigatus*. Infect Immun. 62:5424–5433.

Leitao EA, Bittencourt VC, Haido RM, Valente AP, Peter-Katalinic J, Letzel M, de Souza LM, Barreto-Bergter E. 2003. Beta-galactofuranose-containing *O*-linked oligosaccharides present in the cell wall peptidogalactomannan of *Aspergillus fumigatus* contain immunodominant epitopes. Glycobiology. 13:681–692.

Levery SB, Momany M, Lindsey R, Toledo MS, Shayman JA, Fuller M, Brooks K, Doong RL, Straus AH, Takahashi HK. 2002. Disruption of the glucosylceramide biosynthetic pathway in *Aspergillus nidulans* and *Aspergillus fumigatus* by inhibitors of UDP-Glc: Ceramide glucosyltransferase strongly affects spore germination, cell cycle, and hyphal growth. FEBS Lett. 525:59–64.

Levery SB, Toledo MS, Straus AH, Takahashi HK. 1998. Structure elucidation of sphingolipids from the mycopathogen *Paracoccidioides brasiliensis*: An immunodominant beta-galactofuranose residue is carried by a novel glycosylinositol phosphorylceramide antigen. Biochemistry. 37:8764–8775.

Levery SB, Toledo MS, Straus AH, Takahashi HK. 2001. Comparative analysis of glycosylinositol phosphorylceramides from fungi by electrospray tandem mass spectrometry with low-energy collision-induced dissociation of Li(+) adduct ions. Rapid Commun Mass Spectrom. 15:2240–2258.

Li S, Bao D, Yuen G, Harris SD, Calvo AM. 2007. *bas*A regulates cell wall organization and asexual/sexual sporulation ratio in *Aspergillus nidulans*. Genetics. 176:243–253.

Loureiro y Penha CV, Todeschini AR, Lopes-Bezerra LM, Wait R, Jones C, Mattos KA, Heise N, Mendonca-Previato L, Previato JO. 2001. Characterization of novel structures of mannosylinositolphosphorylceramides from the yeast forms of *Sporothrix schenckii*. Eur J Biochem. 268:4243–4250.

Maciel DM, Rodrigues ML, Wait R, Villas Boas MHS, Tischer CA, Barreto-bergter E. 2002. Glycosphingolipids from *Magnaporthe grisea* cells: Expression of a ceramide dihexoside presenting phytosphingosine as the long-chain base. Arch Biochem Biophys. 405:205–213.

Macura S, Huang Y, Suter D, Ernst RR. 1981. Two-dimensional chemical exchange and cross-relaxation spectroscopy of coupled nuclear spins. J Magn Reson. 43:259–281.

Mille C, Janbon G, Delplace F, Ibata-Ombetta S, Gaillardin C, Strecker G, Jouault T, Trinel PA, Poulain D. 2004. Inactivation of CaMIT1 inhibits *Candida albicans* phospholipomannan beta-mannosylation, reduces virulence, and alters cell wall protein beta-mannosylation. J Biol Chem. 279:47952–47960.

Morelle W, Bernard M, Debeaupuis JP, Buitrago M, Tabouret M, Latgé JP. 2005. Galactomannoproteins of *Aspergillus fumigatus*. Eukaryot Cell. 4:1308–1316.

Nagiec MM, Nagiec EE, Baltisberger JA, Wells GB, Lester RL, Dickson RC. 1997. Sphingolipid synthesis as a target for antifungal drugs. Complementation of the inositol phosphorylceramide synthase defect in a mutant strain of *Saccharomyces cerevisiae* by the AUR1 gene. J Biol Chem. 272:9809–9817.

Petersen BO, Vinogradov E, Kay W, Würtz P, Nyberg NT, Duus JO, Sorensen OW. 2006. H2BC: A new technique for NMR analysis of complex carbohydrates. Carbohydr Res. 341:550–556.

Rance M, Sorensen OW, Bodenhausen G, Wagner G, Ernst RR, Wüthrich K. 1983. Improved spectral resolution in COSY 1H NMR spectra of proteins via double quantum filtering. Biochem Biophys Res Commun. 117:479–485.

Ritchie RG, Cyr N, Korsch B, Koch HJ, Perlin A. 1975. Carbon-13 chemical shifts of furanosides and cyclopentanols. Configurational and conformational influences. Can J Chem. 53:1424–1433.

Rittershaus P, Kechichian TB, Allegood JC, Merril Jr AH, Hennig M, Luberto C, Del Poeta M. 2006. Glucosylceramide synthase in an essential regulator of pathogenicity of *Cryptococcus neoformans*. J Clin Invest. 116:1651–1659.

Sawardeker JS, Sloneker JH, Jeanes A. 1967. Quantitative determination of monosaccharides as their alditol acetates by gas liquid chromatography. Anal Chem. 37:1602–1604.

Suzuki E, Tanaka AK, Toledo MS, Takahashi HK, Straus AH. 2002. Role of beta-D-galactofuranose in *Leishmania major* macrophage invasion. Infect Immun. 70:6592–6596.

Toledo MS, Levery SB, Bennion B, Guimaraes LL, Castle SA, Lindsey R, Momany M, Park C, Straus AH, Takahashi HK. 2007. Sphingolipids of the mycopathogen *Aspergillus fumigatus*: Characterization of glycosylinositol phosphorylceramide antigens with Manp(alpha 1-2)Ins and GlcpN(alpha 1-2)Ins core motifs. J Lipid Res. 48:1801–1824.

Toledo MS, Levery SB, Glushka J, Straus AH, Takahashi HK. 2001. Structure elucidation of sphingolipids from the mycopathogen *Sporothrix schenckii*: Identification of novel glycosylinositol phosphorylceramides with core manalpha1→6Ins linkage. Biochem Biophys Res Commun. 280:19–24.

Toledo MS, Levery SB, Straus AH, Takahashi HK. 2001. Sphingolipids of the mycopathogen *Sporothrix schenckii*: Identification of a glycosylinositol phosphorylceramide with novel core GlcNH(2)alpha1→2Ins motif. FEBS Lett. 493:50–56.

Trinel PA, Maes E, Zanetta JP, Delplace F, Coddeville B, Jouault T, Strecker G, Poulain D. 2002. *Candida albicans* phospholipomannan, a new member of the fungal mannose inositol phosphoceramide family. J Biol Chem. 277:37260–37271.

Tsuji S, Uehori J, Matsumoto M, Suzuki Y, Matsuhisa A, Toyoshima K, Seya T. 2001. Human intelectin is a novel soluble lectin that recognizes galactofuranose in carbohydrate chains of bacterial cell wall. J Biol Chem. 276:23456–23463.

Wagner G. 1983. Two-dimensional relayed coherence transfer spectroscopy of a protein. J. Magn Reson. 55:151–156.

Willker W, Leibfritz D, Kerssebaum R, Bermel W. 1993. Gradient selection in inverse heteronuclear correlation spectroscopy. Magn Reson Chem. 31:287–292.

Wishart DS, Bigam CG, Yao J, Abildgaard F, Dyson HJ, Oldfield E, Markley JL, Sykes BD. 1995. ^{1}H, ^{13}C and ^{15}N chemical shift referencing in biomolecular NMR. J Biomol NMR. 6:135–140.

Zhong W, Jeffries MW, Georgopapadakou NH. 2000. Inhibition of inositol phosphorylceramide synthase by aureobasidin A in *Candida* and *Aspergillus* species. Antimicrob Agents Chemother. 44:651–653.